The Astrophysical Journal, 705:L199–L203, 2009 November 10 doi:10.1088/0004-637X/705/2/L199

EVIDENCE FOR INTERMEDIATE-AGE STELLAR POPULATIONS IN EARLY-TYPE GALAXIES FROM *K*-BAND SPECTROSCOPY

E. Mármol-Queraltó[1], N. Cardiel[1], P. Sánchez-Blázquez[2], S. C. Trager[3], R. F. Peletier[3], H. Kuntschner[4], D. R. Silva[5], A. J. Cenarro[2], A. Vazdekis[2], and J. Gorgas[1]

[1] Dpto. de Astrofísica, Universidad Complutense de Madrid, E28040, Madrid, Spain; emq@astrax.fis.ucm.es
[2] Instituto de Astrofísica de Canarias. c/Vía Láctea S/N, E38205, La Laguna, Tenerife, Spain
[3] Kapteyn Astronomical Institute, University of Groningen, Postbus 800,9700 Av Groningen, Netherlands
[4] Space Telescope—European Coordinating Facility, Karl-Schwarzschild-Str. 2, D-85748 Garching, Germany
[5] National Optical Astronomy Observatory, 950 North Cherry Avenue, Tucson, AZ, 85719, USA
Received 2009 June 10; accepted 2009 September 28; published 2009 October 26

ABSTRACT

The study of stellar populations in early-type galaxies in different environments is a powerful tool for constraining their star formation histories. This study has been traditionally restricted to the optical range, where dwarfs around the turn-off and stars at the base of the red giant branch dominate the integrated light at all ages. The near-infrared spectral range is especially interesting since in the presence of an intermediate-age population, asymptotic giant branch stars are the main contributors. In this Letter, we measure the near-infrared indices Na I and $D_{\rm CO}$ for a sample of 12 early-type galaxies in low-density environments and compare them with the Fornax galaxy sample presented by Silva et al.. The analysis of these indices in combination with Lick/IDS indices in the optical range reveals that (1) the Na I index is a metallicity indicator as good as C4668 in the optical range, and (2) $D_{\rm CO}$ is a tracer of intermediate-age stellar populations. We find that low-mass galaxies in low-density environments show higher Na I and $D_{\rm CO}$ than those located in the Fornax cluster, which points toward a late stage of star formation for the galaxies in less dense environments, in agreement with results from other studies using independent methods.

Key words: galaxies: clusters: general – galaxies: elliptical and lenticular, cD – galaxies: evolution – galaxies: formation – galaxies: stellar content

1. INTRODUCTION

For the majority of galaxies in the universe, the analysis of the stellar content is restricted to the integrated light of their stellar populations, where a small percentage of luminous stars can change the spectra dramatically and bias the final results. A way to overcome this bias is to use a multiwavelength approach, since the fractional contribution from different stars varies along the spectral range. However, most of the observational effort has focused on the optical range, mainly due to the scarcity of appropriate instrumentation in other spectral regions. Especially interesting is the study of the near-infrared (near-IR) window, where red supergiants in young populations (<1 Gyr), asymptotic giant branch (AGB) stars in intermediate-age populations (∼1–2 Gyr), and the tip of the red giant branch (RGB) stars in the near-IR are the main contributors, as opposed to turn-off dwarfs and stars at the lower part of the RGB in the optical. Thus, near-IR spectroscopy may allow a breaking of the degeneracy between multiple stellar populations that plagues optical absorption-line strength studies (e.g., Trager et al. 2000; Sánchez-Blázquez et al. 2006b). In addition, the near-IR wavelength range is less affected by line blanketing effects than other spectral intervals.

Mármol-Queraltó et al. (2008, hereafter MQ08) presented a detailed study of the CO band at 2.3 μm as a function of the basic stellar atmospheric parameters (effective temperature, surface gravity, and metallicity) using a new spectral library of stars in the *K* band. This work confirmed that this CO absorption band is sensitive to metallicity and it also shows good evidence for increased CO absorption strength in AGB stars compared to non-AGB stars (see Figure 14 in MQ08 and Figure 1 in this Letter). These results confirm the suitability of the CO index for stellar population studies. Furthermore, in this spectral range there is a prominent absorption feature at 2.2 μm mainly due to sodium and scandium (Wallace & Hinkle 1996). This feature is very sensitive to the effective temperature of the stars. Once that parameter is fixed, AGB and RGB stars show very similar values (see Figure 1).

The study of galaxies in different environments is a powerful tool to understand their evolution and star formation history (e.g., Sánchez-Blázquez et al. 2003, hereafter SB03; Kuntschner et al. 2002; Thomas et al. 2005; Sánchez-Blázquez et al. 2006a; Collobert et al. 2006). In this Letter, we investigate possible differences in their stellar populations comparing the more prominent absorption features in the *K* band. Only a few detailed studies have been presented in this spectral range after the pioneering photometric work by Frogel et al. (1978) and Aaronson et al. (1978) on early-type galaxies. The first detailed spectroscopic analysis in the *K* band of these galaxies depending on their environment was presented by Mobasher & James (1996), who used the strength of the first CO band at 2.3 μm as an indicator of the presence of AGB stars and, therefore, of an intermediate-age population in elliptical galaxies. They explored the influence of environment finding, initially, a systematic difference between field and cluster galaxies that was later contradicted in James & Mobasher (1999), when the authors enlarged their sample. They also studied the CO strength in Coma cluster galaxies (Mobasher & James 2000), finding variations in the strength of this feature as a function of cluster-centric distance, with more distant galaxies showing deeper CO absorption.

Silva et al. (2008, hereafter S08) observed a sample of 11 early-type galaxies (see Table 1) in the Fornax cluster, and analyzed several line-strength indices (Na I, Ca I, ⟨Fe I⟩, and CO) in the *K* band. For those galaxies showing no trace of young or intermediate-age populations, they found a strong correlation

Table 1
Measurements for the Early-type Galaxies in This Study

Galaxy	Type	Hβ[a] (Å)	Mgb[a] (Å)	C4668[b] (Å)	Na I (Å)	D_{CO}	σ[d] (km s^{-1})	Environment[e]
NGC 3605	E4-5	2.03 ± 0.10	3.83 ± 0.15	6.70 ± 0.30	3.46 ± 0.08	1.2028 ± 0.0016	59.1 ± 7.0	Low density
NGC 3818	E5	1.52 ± 0.05	4.47 ± 0.09	8.20 ± 0.21	4.75 ± 0.12	1.2196 ± 0.0025	199.5 ± 20.7	Low density
NGC 4261	E2-3	1.63 ± 0.05	4.83 ± 0.12	8.71 ± 0.21	5.10 ± 0.26	1.2107 ± 0.0022	300.9 ± 29.4	Low density
NGC 4564	E6	1.60 ± 0.05	5.19 ± 0.11	10.01 ± 0.20	5.68 ± 0.14	1.2314 ± 0.0019	184.3 ± 24.8	Low density
NGC 4636	E-S0	1.53 ± 0.09	5.16 ± 0.15	7.45 ± 0.41	4.03 ± 0.14	1.2138 ± 0.0019	221.2 ± 23.7	Low density
NGC 4742	E4	3.30 ± 0.11	2.67 ± 0.11	5.72 ± 0.20	4.16 ± 0.03	1.2246 ± 0.0009	89.2 ± 9.6	Low density
NGC 5796	E	1.50 ± 0.07	5.39 ± 0.16	8.97 ± 0.23	5.48 ± 0.21	1.2212 ± 0.0021	305.4 ± 22.3	Low density
NGC 5813	E1-2	1.59 ± 0.05	4.66 ± 0.12	7.53 ± 0.21	4.01 ± 0.14	1.2099 ± 0.0021	226.7 ± 25.7	Low density
NGC 5831	E3	1.99 ± 0.15	4.16 ± 0.12	8.43 ± 0.22	4.95 ± 0.08	1.2220 ± 0.0019	151.0 ± 14.5	Low density
ESO382-G16	E	1.42 ± 0.11	4.94 ± 0.15	···	4.61 ± 0.14	1.2115 ± 0.0021	249.2 ± 21.0	Low density
ESO446-G49	S0	1.78 ± 0.12	3.81 ± 0.14	···	4.00 ± 0.11	1.2188 ± 0.0027	118.2 ± 12.6	Low density
ESO503-G12	E	1.86 ± 0.10	3.59 ± 0.13	···	3.87 ± 0.08	1.2207 ± 0.0016	150.1 ± 17.9	Low density
NGC 1316	S0pec	2.39 ± 0.11	4.01 ± 0.13	8.02 ± 0.19	4.61 ± 0.15	1.2258 ± 0.0015	226.0 ± 8.0	Fornax
NGC 1344	E5	2.14 ± 0.09	3.85 ± 0.10	···	4.33 ± 0.15	1.2103 ± 0.0005	171.0 ± 8.0	Fornax
NGC 1374	E0	1.56 ± 0.15	5.04 ± 0.20	7.07 ± 0.24	4.12 ± 0.13	1.2136 ± 0.0006	196.0 ± 9.0	Fornax
NGC 1375	S0	2.93 ± 0.12	2.62 ± 0.16	4.93 ± 0.22	3.50 ± 0.23	1.1952 ± 0.0006	70.0 ± 9.0	Fornax
NGC 1379*	E0	1.68 ± 0.12	4.43 ± 0.15	5.16 ± 0.23	2.87 ± 0.19	1.1967 ± 0.0006	130.8 ± 8.2	Fornax
NGC 1380	S0a	1.70 ± 0.15	4.85 ± 0.21	8.50 ± 0.29	4.51 ± 0.10	1.2062 ± 0.0002	213.0 ± 6.0	Fornax
NGC 1381	S0	1.63 ± 0.09	4.32 ± 0.12	5.99 ± 0.16	3.32 ± 0.15	1.2083 ± 0.0005	169.0 ± 8.0	Fornax
NGC 1399	E0	1.29 ± 0.16	5.98 ± 0.24	8.93 ± 0.39	5.42 ± 0.23	1.2036 ± 0.0022	360.0 ± 8.0	Fornax
NGC 1404*	E2	1.46 ± 0.11	4.95 ± 0.15	8.52 ± 0.24	4.78 ± 0.08	1.2163 ± 0.0006	222.2 ± 7.7	Fornax
NGC 1419	E0	1.62 ± 0.18	3.97 ± 0.23	4.97 ± 0.24	2.86 ± 0.17	1.1982 ± 0.0004	128.0 ± 6.0	Fornax
NGC 1427	E4	1.58 ± 0.08	4.33 ± 0.11	6.20 ± 0.14	3.43 ± 0.17	1.2012 ± 0.0004	186.0 ± 11.0	Fornax

Notes.
[a] Hβ and Mgb indices measured on the optical spectra, extracted within $1/8R_{\rm eff}$, by SB03 and Kuntschner (2000).
[b] C4668 index. New measurements on the optical spectra extracted within $1/8R_{\rm eff}$ by SB03 and original data for Fornax galaxies (Kuntschner 2000).
[d] Central velocity dispersion derived from the near-infrared data by S08 and E. Mármol-Queraltó et al. (2009, in preparation).
[e] Following the criteria in Sánchez-Blázquez et al. (2006a) and Kuntschner et al. (2002).
* Fornax galaxies also observed in this study.

between Na I and CO with velocity dispersion (σ), as well as between those indices and the optical metallicity indicator [MgFe]′ (Thomas et al. 2003). However, the galaxies with young populations in their sample separate from the global trends. More recently, Cesetti et al. (2009) obtained low-resolution spectra for 14 early-type galaxies and confirmed the relation between the near-IR and the optical features.

To unravel possible differences in the stellar content of galaxies in different environments, we analyze a sample of elliptical galaxies located in low-density environments (hereafter *field* galaxies[6]) in comparison with the Fornax galaxy sample presented by S08. This Letter presents the first results of this spectroscopic study, focusing on the Na I and the CO indices. The rest of the indices, as well as a detailed description of the data reduction, will be presented in a forthcoming paper (E. Mármol-Queraltó et al. 2009, in preparation). In Section 2 we describe the data used in this study, while the results and discussion are presented in Sections 3 and 4, respectively. Finally, in Section 5 we present the main conclusions derived from this work.

2. THE DATA

Long-slit spectra for 12 early-type field galaxies (see Table 1) from the samples of Sánchez-Blázquez et al. (2006a) and Kuntschner et al. (2002) plus 2 Fornax galaxies from S08 (for comparison purposes) were obtained with the ISAAC near-IR imaging spectrometer mounted at 8.2 m UT1/Antu telescope at Cerro de Paranal (Chile) with exactly the same instrumental configuration employed by S08. Thus, both samples can be readily compared. The field galaxy sample was chosen to cover a range in σ similar to that spanned by S08's Fornax sample. The spectrometer was used in medium-resolution mode (SWS1 – MR), providing a resolution of 7.1 Å at 2.3 μm (FWHM) with a reciprocal dispersion of 1.21 Å pixel^{-1} for a $120'' \times 1''$ slit. The central wavelength was chosen for each galaxy to include both Na I features and the first CO band (∼2.20 μm and ∼2.29 μm at rest frame, respectively). For each object, several exposures along the slit (A and B positions) were taken for sky subtraction, as is the usual practice for infrared observations. The slit was oriented along the minor axis of the galaxies when possible. After each galaxy set, a nearby A-type star was observed for relative flux calibration and telluric correction. Finally, halogen lamps (on and off) and arc lamps were observed for flat-fielding, and C-distortion correction and wavelength calibration, respectively.

We carried out a standard data reduction in the infrared using REDUCEME (Cardiel 1999). The details of the process will be presented in a forthcoming paper. Galaxy spectra were extracted within a radius corresponding to $1/8R_{\rm eff}$ at the observed position angle for each galaxy, where $R_{\rm eff}$ is the effective radius.

We measured the Na I index (Frogel et al. 2001) and the D_{CO} index (MQ08). The Na I measurements were corrected for broadening effects using the σ-correction computed by S08, while the D_{CO} index is almost insensitive to this effect (see MQ08). In Table 1 we list these measurements for all the galaxies, together with the central velocity dispersion (σ)

[6] This sample includes two galaxies in the Virgo cluster. SB03 showed that there is no difference in their optical indices when comparing them with more isolated galaxies, and for that reason they have been included here.

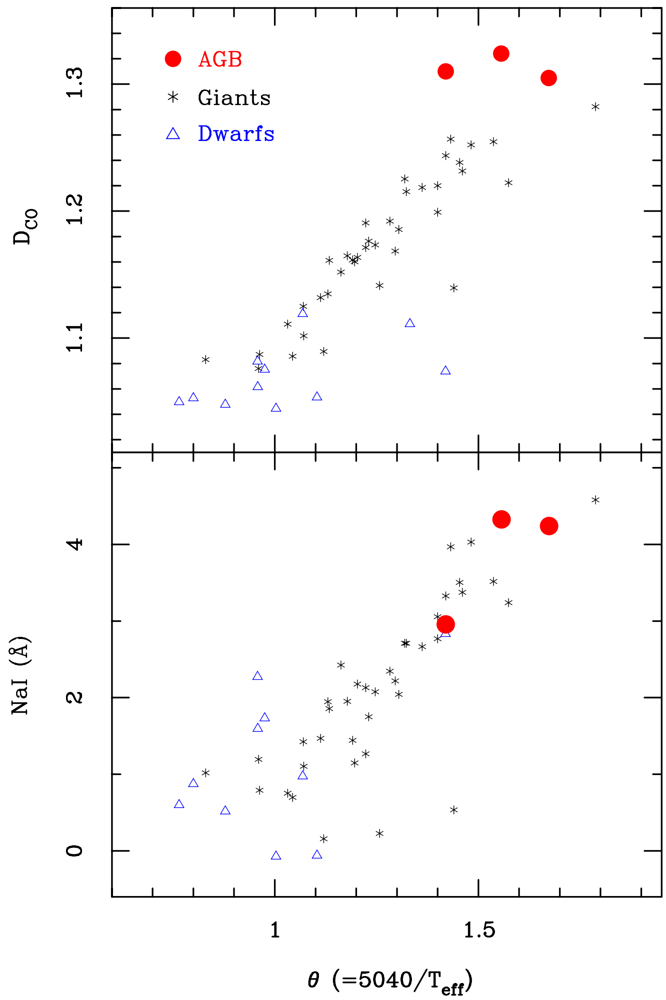

Figure 1. Na I and D_{CO} indices as a function of $\theta = 5040/T_{eff}$ for the subsample of the *K*-band stellar library of MQ08 with the highest quality spectra. The meaning of symbols and colors is explained in the inset. The AGB stars have higher D_{CO} values than giants, while this behavior is not observed in the Na I index.

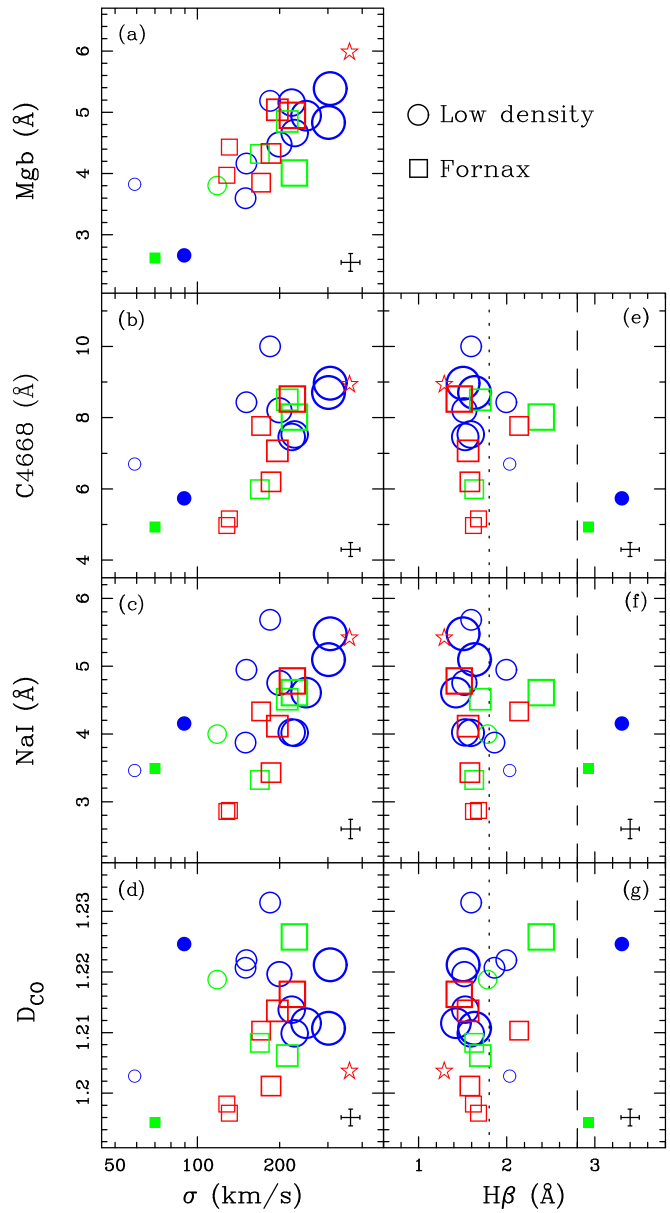

Figure 2. Left column: line-strength indices versus σ for the galaxies analyzed in this Letter (data in Table 1). Right column: line-strength indices versus Hβ index. The dashed line indicates the limit for considering very young galaxies in the blue spectral range. The dotted line shows the limit for H$\beta > 1.8$ Å. Blue circles correspond to galaxies in the field, while red squares represent Fornax cluster galaxies. S0 galaxies of both samples are plotted in green. The two galaxies with the highest Hβ values are marked with filled symbols. The star represents the cD galaxy NGC 1399 (see Lyubenova et al. 2008, for an extensive study of this object in the infrared). Symbol size increases according to the central velocity dispersion of the galaxies.

computed for each galaxy from these infrared spectra. Previous optical work is available for all galaxies. The optical Lick/IDS indices Mgb, C4668, and Hβ were measured on the spectra extracted within a radius corresponding to $1/8R_{eff}$ in the original data by Sánchez-Blázquez et al. (2003; see also Sánchez-Blázquez et al. 2006a) for the field galaxies. For Fornax cluster galaxies, Mgb and Hβ were taken from S08 (measured on the spectra extracted within $1/8R_{eff}$) and C4668 from Kuntschner (2000; original data). All these optical indices have also been included in Table 1.

3. RESULTS

Since there are no reliable stellar population models available describing the behavior of the near-IR indices used in this study, we will interpret the measured features by comparing them with other, better understood, indices. Due to the very strong correlation between metallicity and σ for Fornax elliptical galaxies (Kuntschner 2000), we use σ as a "proxy" for global metallicity in these galaxies. As a "proxy" for the mean age, we will use the Hβ index, which is an indicator of the temperature of the turn-off and, therefore, mainly sensitive to the presence of young stellar populations (between $\sim 2 \times 10^8$ and 10^9 yr; e.g. Allard et al. 2006). Figure 2 shows the behavior of different indices against σ (left column) and Hβ (right column). We note that the number of galaxies analyzed here is small and, therefore, our results might not necessarily apply to all early-type galaxies.

There is a clear correlation between the indices Mgb, C4668, Na I, D_{CO}, and σ for the Fornax galaxies (already shown by Kuntschner 2000 for the optical indices and S08 for the near-IR features). For the field sample, the indices Mgb, C4668 and Na I are also correlated with σ, and these relations exhibit a larger scatter than those obtained for the Fornax sample (see a quantitative statistical analysis of all these diagrams in Table 2). We do not find differences in the Mgb measurements between both galaxy samples, while field galaxies exhibit higher C4668,

Table 2
Statistical Analysis of the Correlations for Field and Fornax Galaxies

Diagram	Low Density			Fornax		
	r_S	α	s_r	r_S	α	s_r
Figure 2(a): Mgb–σ	0.7636	0.0031	0.6685	0.5636	0.0449	0.4764
Figure 2(b): C4668–σ	0.6455	0.0160	1.0440	0.9273	5E−05	0.3287
Figure 2(c): Na I–σ	0.6091	0.0233	1.4256	0.9515	1E−05	0.2165
Figure 2(d): D_{CO}–σ	−0.0545[a]	0.4367	2.7721	0.5757	0.0408	1.5668
Figure 3(a): Na I–C4668	0.9818	4E−08	0.0531	0.9879	5E−08	0.0787
Figure 3(b): D_{CO}–C4668	0.5182	0.0512	0.8005	0.5394	0.0538	1.6243
Figure 3(c): D_{CO}–Na I	0.5727	0.0328	1.0957	0.6000	0.0333	1.9062

Notes.
For each diagram, indicated in the first column of this table, the Spearman rank correlation coefficient r_S and the associated significance level α are given, separately, for the field and Fornax subsamples. In all the cases, the two galaxies with higher Hβ values (filled symbols in the diagrams) have been excluded. With the aim of comparing the scatter observed in each galaxy subsample the residual standard deviation s_r has also been determined as the mean quadratic distance from a linear fit to the data points. Since the data have uncertainties in both axes, the fits have been computed using an ordinary least squares (OLS) bisector method (Isobe et al. 1990). The data ranges were previously renormalized for the proper measure of the perpendicular distances from the data to the fitted straight lines. This renormalization prevents the different weighting introduced by the absolute values of the data. Note that, despite the relations between the indices are evident from the figures, some correlations are not significant due to size of the samples.
[a] If the field galaxy with lowest σ, NGC 3605, is also excluded, we obtain $r_S = -0.4061$ ($\alpha = 0.1221$). Regarding its position in the Mgb– and C4668−σ diagrams, this galaxy could belong to the new family of high-metallicity low-luminosity galaxies found by Sansom & Northeast (2008).

Na I, and D_{CO} indices than Fornax galaxies at $\sigma < 200$ km s^{-1}, with the largest differences for the CO feature. This behavior indicates that there are differences in the star formation history and the metal enrichment between both galaxy samples. As we will discuss below, we are likely seeing the effect of more metal rich intermediate-age stellar populations in these field galaxies, which are not present in most of their Fornax counterparts (S08). For galaxies with higher σ, both samples seem to follow the same trend.

In the right column of Figure 2 we compare different indices with Hβ. We do not find any correlation. Two of the galaxies—marked in all the plots with filled symbols—show very high Hβ indices. These galaxies deviate from all the relations defined by the indices and other parameters. In addition, there are several galaxies with 1.8 Å $<$ Hβ $<$ 2.8 Å, while the bulk of the galaxies have lower Hβ indices. S08 already showed the presence of a small amount of intermediate-age population in the three Fornax galaxies with H$\beta > 1.8$ Å.

Since we find differences in C4668, Na I, and D_{CO} between galaxies in low-density environments and in the Fornax cluster, we explore possible dependences among these indices in Figure 3. The most interesting result is the extremely tight correlation between Na I and C4668 indices in Figure 3(a). This is remarkable given the fact that the indices have been measured on completely independent spectra processed by different authors in distinct spectral ranges. Interestingly, the two galaxies with highest Hβ separate from the global trend. Finally, there are also correlations between D_{CO} and the indices C4668 and Na I (Figures 3(b) and 3(c); see Table 2).

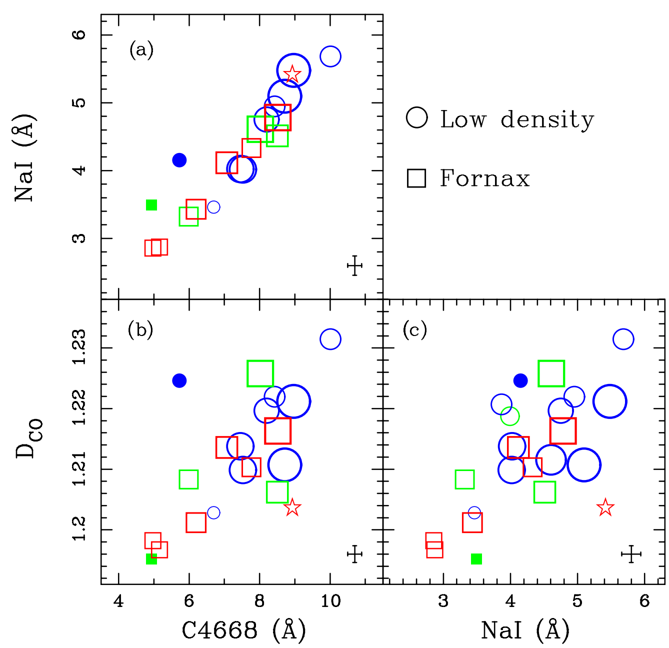

Figure 3. Index–index diagrams for the galaxies in this study. Symbols are explained in Figure 1.

4. DISCUSSION

The main two results of this work are (1) the excellent correlation between the Na I and C4668 indices, and (2) the higher D_{CO} and Na I values in the low-sigma field galaxies compared with their Fornax counterparts. How can we interpret these results in terms of physical parameters? To answer this question, we need to take into account the known dependences of the indices to several parameters. We have to warn the reader that this section is rather speculative, because of the lack of stellar population models in this wavelength region. We should also note that a simple discussion in terms of simple stellar populations (SSPs) is inadequate here, since, as we will discuss, the measured indices in Fornax and field galaxies are very likely indicating differences in their star formation history.

First we describe the qualitative behavior of the indices. For an old SSP, we deduce from the work by MQ08 that D_{CO} increases as a function of metallicity. For younger stellar populations,

D_{CO} increases due to the presence of AGB stars. The Na I index increases with metallicity for old stellar populations (see S08). In S08 it was also shown that Na I increases when a young population is present in the galaxy (see Figure 16 in that paper). Mgb and C4668, like the rest of the non-Balmer indices in the Lick system, are weaker in younger stellar populations (e.g., Vazdekis et al. 2003; Bruzual & Charlot 2003; Thomas et al. 2003; Schiavon 2007). These indices are also sensitive to metallicity, with higher values for more metal-rich populations.

How to explain the behavior of the line indices shown in Figure 2? Following previous studies analyzing galaxies in different environments (e.g., SB03 Trager et al. 2000; Kuntschner et al. 2002; Thomas et al. 2005; Sánchez-Blázquez et al. 2006a, 2006b; Collobert et al. 2006), we start with the assumption that the differences between the field and Fornax samples could be due to distinct star formation histories. As Kuntschner (2000) showed for the Fornax cluster, elliptical galaxies and lenticulars of high σ form an almost coeval family of galaxies, and they exhibit a wide range in metallicity which explains the good correlation of all the indices with σ. On the other hand, previous works have suggested an extended star formation history in field galaxies (e.g., SB03 Collobert et al. 2006; Toloba et al. 2009). If this is the case, we would expect two effects. (1) The chemical enrichment of the interstellar medium produced by previous generations of stars. As a result, the new generation of stars will be more metal rich than the previous ones. (2) The presence of AGB stars from the intermediate-age population of recent star formation episodes.

The higher D_{CO} values for field galaxies with $\sigma < 200\ \mathrm{km\ s^{-1}}$ can be explained by a late stage star formation in these galaxies, which is reflected in a more metal rich population and the presence of AGB stars. Since this index has a positive response to both effects, the differences between field and Fornax galaxies are more prominent here than in other indices. In addition, the more metal rich population in field galaxies would be responsible for the high values of Na I and C4668 in these objects (see Figures 2(b) and (c) and Figures 3(a)–(c)), since both indices are very sensitive to metallicity. Actually, the excellent correlation between Na I and C4668 shown in Figure 3(a) might be indicating that the effect of an intermediate-age population in these two indices is less important, and, therefore, they are both excellent metallicity indicators for old and intermediate ages. However, the two galaxies with the highest Hβ separate from the global trend, as expected due to the sensitivity of these indices to the presence of very young and more metal rich stars, as explained above. The larger scatter in D_{CO} versus C4668 diagram (Figure 3(b)) can be explained by considering that D_{CO} is sensitive to the presence of AGB stars, contrary to the optical C4668 index. Last, both galaxy samples exhibit a similar Mgb index. This is explained by the age–metallicy degeneracy described in previous works (e.g., Worthey et al. 1992; Pedraz et al. 1998; Jørgensen et al. 1999; Kuntschner et al. 2001).

5. CONCLUSIONS

This work has shown the crucial role that the near-IR line-strength indices can play in the understanding of the star formation histories of early-type galaxies. Although interpreting these near-IR indices is difficult without models and the analyzed galaxy samples are still small, we have demonstrated that the measurement of line-strength indices in the near-IR is a useful tool to constrain the star formation histories of these galaxies. In particular, the Na I index has been shown to be a metallicity indicator as good as C4668 in the optical range, while the D_{CO} index can be used as a tracer of intermediate-age stellar populations. The differences in C4668, Na I, and D_{CO}, when studying low-mass galaxies in Fornax cluster and in low-density environments, can be interpreted as field galaxies having undergone later stellar formation episodes than Fornax galaxies. Once synthesis stellar population models in the near-IR range are available, more detailed and quantitative predictions will be made using this interesting wavelength region.

The authors acknowledge the referee, Bahram Mobasher, for his useful comments. E.M.-Q. acknowledges the SMES for a FPI PhD fellowship. This work has been partially supported by the SMES through the research project AYA2007-67752-C03-01. N.C. also acknowledges financial support from the research project AYA2006-15698-C02-02. P.S.-B. acknowledges the financial support from a Marie Curie European Reintegration Grant within the 7th European Community Framework Programme.

Facilities: VLT:Antu (ISAAC)

REFERENCES

Aaronson, M., Cohen, J. G., Mould, J., & Malkan, M. 1978, ApJ, 223, 824
Allard, E. L., Knapen, J. H., Peletier, R. F., & Sarzi, M. 2006, MNRAS, 371, 1087
Bruzual, G., & Charlot, S. 2003, MNRAS, 344, 1000
Cardiel, N. 1999, PhD thesis, Universidad Complutense de Madrid
Cesetti, M., et al. 2009, A&A, 497, 41
Collobert, M., Sarzi, M., Davies, R. L., Kuntschner, H., & Colless, M. 2006, MNRAS, 370, 1213
Frogel, J. A., Persson, S. E., Matthews, K., & Aaronson, M. 1978, ApJ, 220, 75
Frogel, J. A., Stephens, A., Ramírez, S., & De Poy, D. L. 2001, AJ, 122, 1896
Isobe, T., Feigelson, E. D., Akritas, M. G., & Babu, G. J. 1990, ApJ, 364, 104
James, P. A., & Mobasher, B. 1999, MNRAS, 306, 199
Jørgensen, I., Franx, M., Hjorth, J., & van Dokkum, P. G. 1999, MNRAS, 308, 833
Kuntschner, H. 2000, MNRAS, 315, 184
Kuntschner, H., Lucey, J. R., Smith, R. J., Hudson, M. J., & Davies, R. L. 2001, MNRAS, 323, 615
Kuntschner, H., Smith, R. J., Colless, M., Davies, R. L., Kaldare, R., & Vazdekis, A. 2002, MNRAS, 337, 172
Lyubenova, M., Kuntschner, H., & Silva, D. R. 2008, A&A, 485, 425
Mármol-Queraltó, E., Cardiel, N., Cenarro, A. J., Vazdekis, A., Gorgas, J., Pedraz, S., Peletier, R. F., & Sánchez-Blázquez, P. 2008, A&A, 489, 885 (MQ08)
Mobasher, B., & James, P. A. 1996, MNRAS, 280, 895
Mobasher, B., & James, P. A. 2000, MNRAS, 316, 507
Pedraz, S., Gorgas, J., Cardiel, N., & Guzmán, R. 1998, Ap&SS, 263, 159
Sánchez-Blázquez, P., Gorgas, J., Cardiel, N., Cenarro, J., & González, J. J. 2003, ApJ, 590, L91 (SB03)
Sánchez-Blázquez, P., Gorgas, J., Cardiel, N., & González, J. J. 2006a, A&A, 457, 787
Sánchez-Blázquez, P., Gorgas, J., Cardiel, N., & González, J. J. 2006b, A&A, 457, 809
Sansom, A. E., & Northeast, M. S. 2008, MNRAS, 387, 331
Schiavon, R. P. 2007, ApJS, 171, 146
Silva, D. R., Kuntschner, H., & Lyubenova, M. 2008, ApJ, 674, 194 (S08)
Thomas, D., Maraston, C., & Bender, R. 2003, MNRAS, 339, 897
Thomas, D., Maraston, C., Bender, R., & Mendes de Oliveira, C. 2005, ApJ, 621, 673
Toloba, E., Sánchez-Blázquez, P., Gorgas, J., & Gibson, B. K. 2009, ApJ, 691, L95
Trager, S. C., Faber, S. M., Worthey, G., & González, J. J. 2000, AJ, 120, 165
Vazdekis, A., Cenarro, A. J., Gorgas, J., Cardiel, N., & Peletier, R. F. 2003, MNRAS, 340, 1317
Wallace, L., & Hinkle, K. 1996, ApJS, 107, 312
Worthey, G., Faber, S. M., & Gonzalez, J. J. 1992, ApJ, 398, 69